Theory of strain-amplitude–dependent dislocation damping in the presence of uniform point-defect dragging

T. Ö. Oğurtani and A. Seeger
Institut für Physik, Max-Planck-Institut für Metallforschung, D-7000 Stuttgart 80, West Germany
and Metallurgical Engineering Department, Middle East Technical University, Inönü Bulvari, Ankara, Turkey
(Received 12 October 1982)

The strain-amplitude- and frequency-dependent internal friction due to the movements of dislocation of uniform point-defect dragging and randomly distributed weak obstacles is investigated analytically as well as numerically using the string model. By making use of the computer simulations in regard to the catastrophic breakaway distribution function combined with the uniform point-defect dragging model, the internal friction coefficient is obtained as a function of the stress amplitude, the homologous temperature, the driving frequency, and the mean line densities of the dragging point defects and the weak pinning obstacles, respectively. It has been observed by computer experiments that the frequency dependence is solely associated with the point-defect dragging, which also shows strong temperature dependence. Similarly, there is a strong maximum in the decrement—versus—stress-amplitude plot especially for the preferentially oriented single crystal at very low frequencies. On the other hand, the decrement—versus—homologous-temperature plot reveals the existence of two distinct peaks; the dragging and the depinning peaks, respectively, under the appropriate conditions.

I. INTRODUCTION

The effect of large stress amplitudes on the decrement associated with the dislocation damping phenomena has been discussed with partial success in models based upon the mechanical depinning of dislocations from weak pinning-point obstacles.[1,2] In the original theory of Granato and Lücke[2] (GL) in regard to the hysteretic damping, not only the effect of dragging point defects is neglected but also some analytical approximations have been introduced that prevent the model from predicting properly even for the moderate stress amplitudes. However, contrary to the common arguments in the literature,[3] one could easily accommodate the effect of temperature into the model, as we will demonstrate later in this paper by adopting temperature-dependent pinning forces.

The most notable shortcoming of the classical string treatment[2] is the omission of the frequency-dependent part of the logarithmic decrement which generates very critical situations at very small and large stress-amplitude regions. Also the statistical loop-length distribution function employed in the GL theory yields an underestimation of the decrement (hysteretic) at the stress amplitudes well below the peak value of the depinning process. At higher stress values the situation worsens according to our extensive computer experiments. In order to obtain a self-consistent theory of the depinning process which is valid for the whole range of stress amplitudes, the statistical distribution function should be kept as exact as possible and it should be utilized precisely in numerical computations.

The thermally activated breakaway of dislocations has been extensively studied by Teutonico, Granato, and Lücke.[3] Similarly, Koiwa and Hasiguti,[4] Peguin and Birnbaum,[5] and Lücke, Granato, and Teutonico[6] tried to find approximate solutions without introducing the dragging defects, as proposed by Simpson and Sosin,[7,8] explicitly into the string model in order to study the influence of temperature, applied stress amplitude, dislocation length, or the number of pinning obstacles.[9] Recently Schwarz performed extensive computer simulation studies[10] using the string model, which is strictly valid for metals of low Peierls barriers,[11,12] by random distribution of weak obstacles including inertial and viscous forces. However, the effect of point-defect dragging and consequently the dependence of the decrement on the frequency is completely neglected or at least underestimated.

In this paper we will give a theory of the dislocation damping in the field of uniform point-defect dragging plus the depinning process for a complete range of stress amplitudes and the excitation frequencies up to the megacycle region using the well-defined statistical distribution function. However, this mathematically rigorous formulation can only be explored with a sufficient accuracy and in detail by computer experiments. Finally, we will also present an analytical treatment which is very well suited for physical arguments and interpretations for small as well as medium stress-amplitude regimes still including the effect of drag and the excitation frequency.

II. FORMAL THEORY OF STRAIN-AMPLITUDE–DEPENDENT DISLOCATION DAMPING

In this section we shall first give a formal treatment of the nonlinear problem of strain-amplitude–dependent damping based on the assumption that the dynamical character of the breakaway process can be represented by a stress-dependent multivalued distribution function $N(l,\tau)$ of the dislocation loop length l between the pinning-point obstacles of finite strength. $N(l,\tau)$ is a

double-valued function of the loop length and it depends upon whether one deals with the increasing or decreasing branch of the applied stress cycle, $N_1(l,\tau)$ and $N_2(l,\tau)$, respectively. The dislocation strain $\epsilon_d(l)$ produced by the loop of length l in a cube of unit dimensions is given by

$$\epsilon_d(l,t)=b\int_0^l \xi(x,t)dx \ , \tag{1}$$

where b is the Burgers vector and $\xi(x,t)$ is the displacement of the dislocation segment from its rest state. Thus the total dislocation strain for a given instantaneous value of the resolved shear stress τ can be written as

$$\epsilon_{j,d}(\tau)=\int_0^\infty \epsilon_{j,d}(l,\tau)N_j(l,\tau)dl \ . \tag{2}$$

In the above relationship the subscripts $j=1,2$ indicate the double-valued character of the strain as well as the quasi-dynamic distribution function of the loop lengths. One should also mention the following trivial, but important, normalization condition:

$$\Lambda=\int_0^\infty lN_j(l,\tau)dl \ , \tag{3}$$

where Λ is the dislocation density. With the use of the real-number representation for the stress and the strain functions, the energy dissipation per cycle per unit volume of the sample may be written as

$$\Delta W=\oint \tau(t)d\epsilon_d(t)=-\oint \epsilon_d(t)d\tau(t) \ , \tag{4}$$

which for a simple harmonic excitation $\tau=\tau_0\sin(\omega t)$ yields

$$\Delta W=-2\left[\int_0^{T/4}\epsilon_{1,d}(t)\partial_t\tau(t)dt+\int_{T/4}^{T/2}\epsilon_{2,d}(t)\partial_t\tau(t)dt\right] \tag{5}$$

or

$$\Delta W=-2\left[\int_0^{\tau_0}\epsilon_{1,d}(\tau)d\tau-\int_0^{\tau_0}\epsilon_{2,d}(\tau)d\tau\right] . \tag{6}$$

Expression (6) is very useful if one deals with the case which is called the strain-amplitude–dependent dislocation damping, but the frequency-independent dislocation damping, for which the dislocation strain $\epsilon_d(\tau)$, as we will show later, is directly proportional with the instantaneous value of τ. Otherwise, the parametric relationship (5) will be very convenient in actual calculations.

The logarithmic decrement can be obtained by the following expression:

$$\delta=\Delta W/2W \ , \tag{7}$$

where W is the total vibrational energy which is given by $\sigma_0^2/2E$, σ_0 is the amplitude of the applied uniaxial stress, and $E(\theta,\phi)$ is the Young's modulus of the single crystal; θ and ϕ are the angles which relate applied stress to resolved shear stress in the slip plane and in the slip direction, respectively. Using the well-known Schmid's transformation $\tau=\sigma R(\theta,\phi)$, one can write

$$\delta(\sigma_0)=E(\theta,\phi)R^2(\theta,\phi)[\Delta W(\tau_0)/\tau_0^2] \ , \tag{8}$$

where $R(\theta,\phi)$ is the Schmid's factor which is given by $R(\theta,\phi)=\cos\theta\sin\theta\cos\phi$. Equation (8) clearly indicates that even in the case of an elastically isotropic single-crystal specimen the decrement still strongly depends upon the orientation of the applied uniaxial stress system with respect to the active dislocation slip system. Similarly, the decrement in terms of the amplitude of the applied uniaxial stress σ_0 will be represented by the following expression:

$$\delta(\sigma_0)=E(\theta,\phi)\Delta W(|R(\theta,\phi)|\sigma_0)/\sigma_0^2 \ , \tag{9}$$

and in the case of the polycrystalline sample with random texture the average value of the decrement can be given by

$$\langle\delta(\sigma_0)\rangle=\int E(\theta,\phi)\Delta W(|R(\theta,\phi)|\sigma_0)\sin\theta\, d\theta\, d\phi/4\pi\sigma_0^2 \ . \tag{10}$$

The relationship (10) can be also given in the following format which clearly emphasizes the individual character of the decrement associated with each active slip system in the crystalline materials:

$$\langle\delta(\sigma_0)\rangle=\sum_i \frac{E(\theta_i,\phi_i)}{G_i}R^2(\theta_i,\phi_i)\delta^i(\tau_0)\Big|_{\tau_0=\sigma_0|R(\theta_i,\phi_i)|} \ , \tag{11}$$

where

$$\delta^i(\tau_0)\equiv\Delta W^i(\tau_0)/G_i^{-1}\tau_0^2 \ . \tag{12}$$

In the above expressions G_i denotes the shear modulus for the ith slip system, and for an isotropic single crystal one has $E=2G(1+\nu)$, where ν is the Poisson's ratio.

III. STRAIN-AMPLITUDE–DEPENDENT DISLOCATION DAMPING IN THE PRESENCE OF POINT-DEFECT DRAGGING

In this section, as far as the main statistical aspect of the distribution function of $N_j(l,\tau)$ is concerned, we will make use of the Koehler-Granato-Lücke (KGL) catastrophic breakaway model which was originally proposed by Koehler[1] and highly refined by Granato and Lücke.[2] However, in the general formulation of the problem, especially for numerical solutions, we will keep the exact form of the probability, M, that a catastrophe has occurred in the network length as

$$M=[1-(q+1)\exp(-q)]^n \tag{13}$$

rather than the one used by the above authors (GL) as a good approximation for the early stages of the breakaway process:

$$M\cong n(q+1)\exp(-q) \ , \tag{14}$$

where $q=L/L_c$, L is the critical breakaway length and L_c is the mean length between the weak pinning points. Here n is the number of weak pinning points in the network length.

According to the KGL model there are two distinct types of pinning points situated along the dislocation line: the network pinning points which have infinite breakaway strength and are uniformly distributed along the dislocation with an average length L_N, and pinning points that are randomly arranged along the dislocation segment and which exhibit finite breakaway strength or the maximum

pinning force denoted by f_m. When the force exerted by the dislocation line on this pinning point is larger than the breakaway force f_m, the so-called catastrophic breakaway process starts and continues until the whole dislocation segment between two strongly pinned network points has broken away completely. The distribution function obtained by Granato and Lücke[2] using Eq. (14) may be summarized, which will be also utilized in this paper later for the analytical solution of certain special problems, as follows:

$$N_1(l,q)=\begin{cases}(\Lambda/L_c^2)[1-n(q+1)\exp(-q)]\exp(-l/L_c)\,, \\ \qquad\qquad 0<l<L<L_N \qquad (15)\\ (\Lambda/L_N)[n(q+1)\exp(-q)]\delta(l-L_N)\,, \\ \qquad\qquad L<l<\infty \qquad (16)\end{cases}$$

and

$$N_2(l,q)=N_1(l,q_0),\quad 0<l<\infty\,. \qquad (17)$$

In addition, one must impose the following condition: If $q\geq\gamma$: $\gamma\rightarrow q$, where $\gamma=L_N/L_c$. This means that the upper limit for the critical breakaway length L is L_N, the dislocation segment length. Similarly, the average value of n is given by $n=(L_N/L_c)-1$ or $n=\gamma-1$.

The critical breakaway length may be given by $L\sim f_m/\tau$, where the exact nature of the proportionality constant depends upon the specific model calculations. According to our analysis $q=\Gamma_c/\tau$, where Γ_c is given by $\pi^2 f_m/4aL_c$ as a first-order approximation.[13,14] Similarly, $q_0=\Gamma_c/\tau_0$.

The mean line density of the weak obstacles is presented by $N_{\rm ob}^d=(n+1)/L_N$ or $N_{\rm ob}^d=\gamma/L_N$, if one uses the conventional definition of $N_{\rm ob}^d\equiv 1/L_c$. Therefore, for a given dislocation network length L_N, the line density of the weak pinning-point defects can be uniquely represented by γ. In computer experiments it is better to normalize the stress amplitude with respect to a quantity defined as $\Gamma_N\equiv\pi^2 f_m/4aL_N$ which is independent from the line density of the weak obstacles, and hence $q=\gamma(\Gamma_N/\tau)$. Physically, $\Gamma_N/2$ corresponds to the minimum-resolved shear stress level necessary for the breakaway of those loops which have lengths equal to the network length L_N.

The exact distribution function can be obtained using Eq. (13) rather than Eq. (14), which is valid for the whole range of stress amplitude and also satisfies the conservation of the dislocation density as described by Eq. (3). Using the statistical arguments along the line of the catastrophic breakaway process as advocated by GL, one obtains the following distribution function which has a wider range of validity, but still assuming that the loop lengths are statistically independent[2]:

$$N_1(l,q<\gamma)=\begin{cases}(\Lambda/L_c^2)[1-(q+1)\exp(-q)]^{n-1}\exp(-l/L_c), & 0\leq l\leq L<L_N\\ (\Lambda/L_N)\{1-[1-(1+q)\exp(-q)]^n\}\delta(l-L_N), & L<l<\infty\end{cases} \qquad (18)$$

and

$$N_1(l,q\geq\gamma)=(\Lambda/L_c^2)\Theta(L_N-l)\exp(-l/L_c)+(\Lambda/L_N)(1+\gamma)e^{-\gamma}\delta(l-L_N)\,, \qquad (19)$$

where $\Theta(z)$ is the Heaviside function defined by $\Theta(z)=\{0,z<0\};\ \{1,z>0\}$. Furthermore, we have $N_2(l,q)=N_1(l,q_0)$ when $0<l<\infty$.

The relationship denoted by Eq. (19) is very interesting and it clearly states the existence of a threshold stress level below which the loop distribution function is completely frozen-in. This threshold stress level as stated previously corresponds to the stress which is just strong enough to break away a dislocation loop of length denoted by L_N which results in $q_{\rm thr}=\gamma$ and $\tau_{\rm thr}=\Gamma_N$. As one might expect from the model, the threshold stress level gives the upper bond for the stress-independent region of dislocation damping as also proved to be the true conclusion by our extensive computer evaluations. This threshold stress level also gives the upper limit of the stress beyond which the linearity between the strain and the stress starts to disappear. The important feature of the distribution function presented by the present authors is that for large values of the stress, $q\rightarrow 0$, Eq. (18) predicts properly that all the loops will be concentrated at $l=L_N$ (the δ function) which cannot be deduced from the relationships Eqs. (15) and (16) introduced by Granato and Lücke.[2] However, for small stresses, Eq. (18) yields the same expressions given by Eqs. (15) and (16) from the binomial expansion keeping the first significant term. Finally, we want to point out that the main reason for the occurrence of the sharp threshold stress level is the fact that the network lengths are assumed to be uniform in value denoted by L_N (the δ distribution). To be more realistic, the model should be further modified in the mathematical treatment to take account of the fact that a distribution of network lengths do occur in nature. For an arbitrary network distribution function $P(L_N)$ the total decrement can be calculated from the following formula:

$$\delta_T=\int_0^\infty[\delta(L_N)/\Lambda_N]L_N P(L_N)dL_N\,, \qquad (20)$$

for a random distribution of network loop lengths one furthermore has

$$P(L_N)=[\Lambda_T/\langle L_N\rangle^2]^{-1}\exp(-L_N/\langle L_N\rangle)\,, \qquad (21)$$

where $\delta(L_N)$ is the decrement obtained assuming that the network points are uniformly arranged along the dislocation line. Λ_N is the dislocation density associated with the network length L_N. Similarly, $\langle L_N\rangle$ is the average network length and Λ_T denotes the total dislocation density. In the present work we shall deal with the calculation of $\delta(L_N)$ only.

A. Dislocation oscillations under the effect of uniform point-defect drag

In addition to the immobile but finite breakaway strength exhibited by point defects (obstacles), we will also

consider those point defects which are highly mobile due to the thermal fluctuations, and exert the viscous drag effect on the moving dislocation segment under the action of the applied stress system. According to the breakaway statistics adopted in the present work, the pinning points due to the immobile impurities are rigid boundary conditions below the certain critical-resolve shear stress value (which can be calculated for a given maximum pinning force f_m in terms of the adjoining loop lengths). Therefore, the unified dislocation damping theory associated with the point-defect dragging developed by Oğurtani[13] is strictly valid in the calculation of the displacement of the dislocation line segment up to the critical-resolve stress level beyond which the catastrophic breakaway or depinning process starts and continues until the whole dislocation segment in question between two network points (or strong obstacles) has broken away. Hence we can write[13] the following expression:

$$\xi_d(l,t)=\mathrm{Im}\left[-\frac{b\tau_0\exp(i\omega t)\alpha^2}{C}\left[1-\frac{\cos[(x-l/2)/\alpha]}{\cos(l/2\alpha)}\right]\right], \tag{22}$$

where $l<L$, and similarly for the dislocation strain

$$\epsilon_d(l,t)=\mathrm{Im}\{-2\tau_0 C^{-1}\exp(i\omega t)\alpha^3 b^2 \times[l/2\alpha-\tan(l/2\alpha)]\}, \tag{23a}$$

where $\alpha^2=iC/\omega(i\omega+d)A$ and $d=B/A$. In the above exact expressions A is the effective mass per unit length of the dislocation segment, C is the line tension which is assumed to be constant along the dislocation line, and B is the effective damping constant associated with uniform drag which can be given by the following relationship[13]:

$$B=B_0+B_d(N_a+1)/l, \tag{23b}$$

where B_0 is the viscous damping constant or coefficient (background damping) in the absence of the mobile defects and B_d is the damping constant for each of the N_a dragging point defects along the dislocation loop of length equal to l. In the case of uniform (continuum-limit) distribution of the mobile defects we can have the following replacements: $B_d=kT/D_a'$ (Einstein-Nernst relationship) and $(N_a+1)/l=n_a^d(T)$, where D_a' is the diffusivity of the mobile dragging defects denoted by a in the immediate vicinity of the dislocation line and n_a^d is the mean-linear density of these defects at the dislocation segment. The temperature dependence of $n_a^d(T)$ is very critical in character and shows a Fermi-Dirac type (or the analog of the Langmuir-adsorption isotherm) functional behavior with low-temperature site saturation (see the Appendix).

In the analytical manipulations of the frequency dependence of the problem, the following Fourier sine series expansion of the closed form [Eqs. (31), (32), and (35) in Ref. 13 should be divided by π] given by Eq. (23) in the interval of $[0,l]$ is very convenient,[13]

$$\epsilon_d(l,t)=\mathrm{Im}\left[\frac{\delta_0\tau_0 e^{i\omega t}}{\pi G}\right]\sum_{m=0}^{\infty}(2m+1)^{-2}\left[\frac{(2m+1)^2-\Omega_A^2}{[(2m+1)^2-\Omega_A^2]^2+\Omega_B^2}-i\frac{\Omega_B}{[(2m+1)^2-\Omega_A^2]^2+\Omega_B^2}\right], \tag{24}$$

where $\delta_0=8Gb^2/\pi^3C$, $\Omega_A=\omega/\omega_A^0$, and $\Omega_B=\omega/\omega_B^0$. ω_A^0 is the fundamental resonance frequency of the dislocation segment which is given by $\omega_A^0=(\pi/l)(C/A)^{1/2}$. Similarly, ω_B^0 is the fundamental resonance frequency of a vibrating dislocation segment without inertia in the viscous media, and it is given by $\omega_B^0=(\pi/l)^2C/B$.

The first summation in Eq. (24) indicates the existence of the linear relationship (in phase) between the plastic strain of a dislocation segment and the instantaneous value of the applied resolved shear stress. In the calculation of the hysteretic dislocation damping which shows only the stress amplitude dependence but not the frequency, the first term in the first sum in Eq. (24) has been used by Granato and Lücke[2] assuming further that Ω_A and Ω_B are identically equal to zero.

The second sum in the above expression (24) which lags 90° behind the excitation corresponds to the energy dissipation which shows also strong frequency dependence. Our extensive computer model experiments have indicated that if one works in the driving frequency range which is less than, e.g., $0.01\omega_A^N$ (for an exponential loop distribution), where $\omega_A^N=(\pi/L_N)(C/A)^{1/2}$ which is almost in the megacycle range, the inertial term Ω_A can be completely neglected in Eq. (24).

Hence up to and including the megacycle range the following expression can be safely used in the representation of the strain associated with the dislocation line segment of length l:

$$\epsilon_d(l,t)\cong\frac{\delta_0\tau_0 l^3}{\pi G}\left[\frac{\sin(\omega t)}{1+\Omega_B^2}-\frac{\Omega_B\cos(\omega t)}{1+\Omega_B^2}\right]. \tag{25}$$

The relationship (25) can also be written in terms of the instantaneous value of the shear stress which shows explicitly two distinct branches whether τ is increasing or decreasing, minus or positive sign in front of the second term, respectively, as follows:

$$\left.\begin{matrix}\epsilon_{1,d}(l,\tau)\\ \epsilon_{2,d}(l,\tau)\end{matrix}\right\}=\frac{\delta_0 l^3}{\pi G}\left[\frac{\tau}{1+\Omega_B^2}\pm\frac{\Omega_B(\tau_0^2-\tau^2)^{1/2}}{1+\Omega_B^2}\right], \tag{26}$$

where Ω_B is a function of the dislocation loop length according to our previous definition, and it may be rewritten in the following normalized fashion:

$$\Omega_B=\Omega_{B,N}(l/L_c)^2\gamma^2 \tag{27}$$

and

$$\Omega_{B,N}\equiv\frac{\omega BL_N^2}{\pi^2 C},$$

to emphasize the loop-length dependence of Ω_B explicitly.

B. Amplitude and the frequency-dependent decrement in general format

In this section we will give the analytical expression for the logarithmic decrement associated with the hysteretic damping which is presented simultaneously with the mobile defect dragging process acting for the whole frequency range of main experimental interest (up to and including the megacycle region), and covering the rather wide stress amplitude span which is somewhat below the operation level of the *F-R* source.

Now and then we will investigate the above-mentioned in-phase and out-phase contributions which will be denoted by the superscript I and II, respectively, as individual and separate terms. From Eqs. (2), (18), (19), and (26) the following can be immediately obtained:

$$\epsilon^{\mathrm{I}}_{1,d}(\tau)=\frac{\delta_0\tau}{\pi G}\int_0^{\infty}\frac{l^3}{1+\Omega_B^2}N_1(l,q)dl\ , \tag{28}$$

hence for $q<\gamma$ or $\tau>\Gamma_N$

$$\epsilon^{\mathrm{I}}_{1,d}(\tau)=\frac{\delta_0\tau}{\pi G}\left[\frac{\Lambda}{L_c^2}[1-(q+1)e^{-q}]^{n-1}\int_0^{L}\frac{l^3e^{-l/L_c}dl}{1+\Omega^2_{B,N}(l/L_c)^4\gamma^{-4}}+\frac{\Lambda}{L_N}\{1-[1-(1+q)e^{-q}]^n\}\frac{L_N^3}{1+\Omega^2_{B,N}}\right], \tag{29}$$

and when $q\geq\gamma$ or $\tau\leq\Gamma_N$

$$\epsilon^{\mathrm{I}}_{1,d}(\tau)=\frac{\delta_0\tau}{\pi G}\left[\frac{\Lambda}{L_c^2}\int_0^{L_N}\frac{l^3e^{-l/L_c}dl}{1+\Omega^2_{B,N}(l/L_c)^4\gamma^{-4}}+\frac{\Lambda}{L_N}(1+\gamma)e^{-\gamma}\frac{L_N^3}{1+\Omega^2_{B,N}}\right], \tag{30}$$

where $L/L_c=\Gamma_c/\tau=q$, $n=\gamma_1$, and $\gamma=L_N/L_c$. Similarly, one has also the following expression for the out phase (90° lagging):

$$\epsilon^{\mathrm{II}}_{1,d}(\tau)=-\frac{\delta_0(\tau_0^2-\tau^2)^{1/2}}{\pi G}\int_0^{\infty}\frac{l^3\Omega_BN_1(l,q)dl}{1+\Omega_B^2}\ , \tag{31}$$

which results for $q<\gamma$ or $\tau>\Gamma_N$,

$$\epsilon^{\mathrm{II}}_{1,d}(\tau)=-\frac{\delta_0(\tau_0^2-\tau^2)^{1/2}}{\pi G}\left[(\Lambda/L_c^2)[1-(q+1)e^{-q}]^{n-1}\int_0^{L}\frac{\gamma^2l^3\Omega_{B,N}(l/L_c)^2e^{-l/L_c}dl}{1+\Omega^2_{B,N}(l/L_c)^4\gamma^{-4}}\right.$$

$$\left.+(\Lambda/L_N)\{1-[1-(1+q)e^{-q}]^n\}\frac{L_N^3\Omega_{B,N}}{1+\Omega^2_{B,N}}\right], \tag{32}$$

and when $q\geq\gamma$ or $\tau\leq\Gamma_N$,

$$\epsilon^{\mathrm{II}}_{1,d}(\tau)=-\frac{\delta_0(\tau_0^2-\tau^2)^{1/2}}{\pi G}\left[(\Lambda/L_c^2)\int_0^{L_N}\frac{\gamma^2l^3\Omega_{B,N}(l/L_c)^2e^{-l/L_c}dl}{1+\Omega^2_{B,N}(l/L_c)^4\gamma^{-4}}+(\Lambda/L_N)(1+\gamma)e^{-\gamma}\frac{L_N^3\Omega_{B,N}}{1+\Omega^2_{B,N}}\right]. \tag{33}$$

For the decreasing part of the stress cycle one may use the following identities:

$$\epsilon^{\mathrm{I}}_{2,d}(\tau)=\epsilon^{\mathrm{I}}_{1,d}(\tau)\,|_{\,q=q_0} \tag{34}$$

and

$$\epsilon^{\mathrm{II}}_{2,d}(\tau)=-\epsilon^{\mathrm{II}}_{1,d}(\tau)\,|_{\,q=q_0}\ . \tag{35}$$

Using the above results in connection with the relationships (6) and (7) the logarithmic decrement can be formulated which after rearrangements takes the following format:

$$\delta=\delta^{\mathrm{I}}+\delta^{\mathrm{II}}\ , \tag{36}$$

where

$$\frac{\delta^{\mathrm{I}}}{\delta_0\Lambda L_N^2}=\frac{|R|^2E}{\pi G}\left[-\frac{2}{x_0^2}\right]\left\{\Theta(\gamma-q)\left[\int_0^{x_0}\frac{[1-(q+1)e^{-q}]^{n-1}}{\gamma^2}\left[\int_0^{q}\frac{y^3e^{-y}}{1+\Omega^2_{B,N}y^4\gamma^{-4}}dy+\frac{1-[1-(1+q)e^{-q}]^n}{1+\Omega^2_{B,N}}\right]x\,dx\right]\right.$$

$$\left.+[1-\Theta(\gamma-q)]\left[\int_0^{x_0}\left[\frac{1}{\gamma^2}\int_0^{\gamma}\frac{y^3e^{-y}}{1+\Omega^2_{B,N}y^4\gamma^{-4}}dy+\frac{(1+\gamma)e^{-\gamma}}{1+\Omega^2_{B,N}}\right]x\,dx\right]\right.$$

$$-\Theta(\gamma-q_0)\frac{x_0^2}{2}\frac{[1-(q_0+1)e^{-q_0}]^{n-1}}{\gamma^2}\left[\int_0^{q_0}\frac{y^3e^{-y}}{1+\Omega_{B,N}^2y^4\gamma^{-4}}dy+\frac{1-[1-(1+q_0)e^{-q_0}]^n}{1+\Omega_{B,N}^2}\right]$$

$$-[1-\Theta(\gamma-q_0)]\frac{x_0^2}{2}\left[\frac{1}{\gamma^2}\int_0^{\gamma}\frac{y^3e^{-y}}{1+\Omega_{B,N}^2y^4\gamma^{-4}}dy+\frac{(1+\gamma)e^{-\gamma}}{1+\Omega_{B,N}^2}\right]\Bigg\}, \tag{37}$$

where $x_0=\tau_0/\Gamma_c$, $q=1/x$, and $q_0=1/x_0$; $\Theta(z)\equiv 1$ for $z>1$ and $\Theta(z)\equiv 0$ for $z\leq 0$.

Similarly, one has the following expression for the out-of-phase contribution to the decrement:

$$\frac{\delta^{II}}{\delta_0\Lambda L_N^2}=\frac{|R|^2E}{\pi G}\left[\frac{2}{x_0^2}\right]\Bigg\{\Theta(\gamma-q)\left[\int_0^{x_0}\frac{[1-(q+1)e^{-q}]^{n-1}}{\gamma^4}\left[\int_0^{q}\frac{\Omega_{B,N}y^5e^{-y}}{1+\Omega_{B,N}y^4\gamma^{-4}}dy\right.\right.$$

$$\left.+\frac{1-[1-(q+1)e^{-q}]^n\Omega_{B,N}}{1+\Omega_{B,N}^2}\right](x_0^2-x^2)^{1/2}dx\Bigg]$$

$$+[1-\Theta(\gamma-q)]\left[\int_0^{x_0}\left[\frac{1}{\gamma^4}\int_0^{\gamma}\frac{\Omega_{B,N}y^5e^{-y}}{1+\Omega_{B,N}^2y^4\gamma^{-4}}dy+\frac{(1+\gamma)e^{-\gamma}\Omega_{B,N}}{1+\Omega_{B,N}^2}\right](x_0^2-x^2)^{1/2}dx\right]$$

$$+\Theta(\gamma-q_0)\frac{\pi x_0^2}{4}\frac{[1-(q_0+1)e^{-q_0}]^{n-1}}{\gamma^4}\left[\int_0^{q_0}\frac{\Omega_{B,N}y^5e^{-y}}{1+\Omega_{B,N}^2y^4\gamma^{-4}}dy+\frac{1-[1-(q_0+1)e^{-q_0}]^n\Omega_{B,N}}{1+\Omega_{B,N}^2}\right]$$

$$+[1-\Theta(\gamma-q_0)]\frac{\pi x_0^2}{4}\left[\frac{1}{\gamma^4}\int_0^{\gamma}\frac{\Omega_{B,N}y^5e^{-y}}{1+\Omega_{B,N}^2y^4\gamma^{-4}}dy+\frac{(1+\gamma)e^{-\gamma}\Omega_{B,N}}{1+\Omega_{B,N}^2}\right]\Bigg\}. \tag{38}$$

The above rigorous expressions for the logarithmic decrement involve certain double integrals which cannot be represented in terms of the well-known special functions. However, they can be studied numerically under the wide range of parametric variations which will be discussed later in this paper. In the following sections we will give an analytical treatment of the linear frequency region as a special case which still contains much information in regard to the damping behavior of dislocations at high stress amplitudes.

C. Amplitude-dependent dislocation damping in the linear frequency region

In the low-frequency range where $\omega<\omega_B^0$ one can obtain the following expression from Eq. (24), or perhaps more easily from the compact and closed relationship (22), which yields ($\Omega_A\rightarrow 0$)

$$\epsilon_d(l,t)\rightarrow\frac{\tau_0b^2l^3}{12C}\left[\sin\omega t-\frac{\omega l^2B}{10C}\cos\omega t\right] \tag{39}$$

or

$$\epsilon_d(l,t)\rightarrow\frac{\delta_0'\tau_0l^3}{\pi G}(\sin\omega t-\Omega_B'\cos\omega t)\,, \tag{40}$$

where $\delta_0'=\pi Gb^2/12C$, $\Omega_B'=\omega/\omega_B^{0\prime}$, and $\omega_B^{0\prime}=10C/Bl^2$. Note the small numerical differences between these newly defined quantities and the analogous ones defined previously. This is due to the fact that in the derivation of Eqs. (39) and (40) we have used the complete infinite series expansion rather than the first terms as has been done in connection with expression (25). However, the numerical differences are extremely small. With the use of Eqs. (2), (9), (15), and (40), the following exact expressions can be derived:

$$\epsilon_{1,d}^{I}(\tau)=\frac{\delta_0}{\pi G}\tau\Lambda L_C^2 3!\left\{1+e^{-q}\left[\gamma^2(\gamma-1)\frac{q+1}{3!}-\left[\frac{q^3}{3!}+\frac{q^2}{2!}+q+1+(\gamma-1)(q+1)\right]\right]\right.$$

$$\left.+(\gamma-1)(q+1)\left[\frac{q^3}{3!}+\frac{q^2}{2!}+q+1\right]e^{-2q}\right\} \tag{41}$$

for $q<\gamma$, *otherwise* $\gamma\rightarrow q$ in the above relationship and

$$\epsilon_{1,d}^{II}(\tau,\omega)=-\frac{\delta_0\Omega_{B,N}(\tau_0^2-\tau^2)^{1/2}}{\pi G}\Lambda\frac{L_N^2}{\gamma^4}5!\left[1+e^{-q}\left\{\gamma^4(\gamma-1)\frac{q+1}{5!}-\left[\left[\sum_{m=0}^{5}\frac{q^m}{m!}\right]+(\gamma-1)(q+1)\right]\right\}\right.$$

$$\left.+(\gamma-1)(q+1)\left[\sum_{m=0}^{5}\frac{q^m}{m!}\right]e^{-2q}\right], \tag{42}$$

for $q<\gamma$; *otherwise* $\gamma\rightarrow q$ (replacement operation) in the above expression, where $\gamma=L_N/L_c$, and it is closely related to the average linear density of the weak obstacles denoted by $N_{\rm ob}^d=1/L_c$ or $N_{\rm ob}^d=\gamma/L_N$. The relationship (41) is very similar to the one obtained by Granato and Lücke[2] with a slightly different numerical factor of $8/\pi^4$ rather than $\frac{1}{12}$. However, the $q\geq\gamma$ case has not been treated explicitly in their paper which causes serious problems if one calculates the logarithmic decrement for small and medium stress levels.

Using the relationships (41) and (42) in connection with Eqs. (6), (7), (34), and (35), one can obtain the internal friction behavior of the system in the linear frequency range as follows:

$$\frac{\delta^{\rm I}}{\delta_0\Lambda L_N^2}=|R|^2E(\pi G)^{-1}[D(q_0)-D(\gamma)]\,, \tag{43}$$

where $q_0<\gamma$; *otherwise* $\gamma\rightarrow q_0$. Furthermore,

$$D(z)\equiv(3!z^2/\gamma^2)\left[-e^{-z}\frac{1+z}{3!}+(\gamma-1)\left[\frac{\gamma^2}{3!}-1\right]E_1(z)+(\gamma-1)\left[\frac{z^2}{3!}+\frac{z}{2!}+\frac{3}{4}\right]e^{-2z}+(\gamma-1)E_1(2z)\right], \tag{44}$$

where $E_1(z)=\int_z^\infty e^{-z}z^{-1}dz$ is the exponential integral[14] function mostly denoted by the notation of $-Ei(-z)$. The relationship (43) is obtained exactly without having any mathematical approximation, only assuming that the distribution function given by Granato and Lücke[2] is valid [see Eqs. (15) and (16) and the imposed condition].

In the above exact relationship the terms which involve $E_1(2z)$ are completely negligible. We should also mention that the stress-amplitude dependence comes from the fact that $q_0=\Gamma_c/\tau_0$, or in terms of the applied uniaxial stress system one has $q_0=\Gamma_c/|R(\theta,\phi)|\sigma_0$. Equation (43) yields an identically equal to zero logarithmic decrement for the stress-amplitude levels below the threshold level which was also stated previously in connection with the rigorous solution, $q_0=\gamma$ or $\tau_{\rm thr}=\Gamma_N$. Well above the threshold level the $D(\gamma)$ term also gives a negligible contribution which can be immediately discarded. However, if one wishes to obtain consistent theory in regard to the temperature dependence, then one must deal with the stress-amplitude–independent region as well as the stress-dependent range simultaneously, therefore in that case the $D(\gamma)$ term should be kept in numerical calculations.

The logarithmic decrement represented by Eq. (43) has a well-defined maximum with respect to the applied uniaxial stress amplitude which can be determined from the following transcendental equation numerically:

$$(\gamma-1)(\gamma^2/3!-1)[2E_1(q_m)-\exp(-q_m)]+(q_m^2-2q_m-2)\exp(-q_m)/3!=0\,, \tag{45}$$

which actually yields a very simple but highly accurate expression for $\gamma>3$, such as

$$2E_1(q_m)-\exp(-q_m)=0\,, \tag{46}$$

which results in $q_{\max}=1.3$. The corresponding peak value of the logarithmic decrement may be immediately written using this finding:

$$\left.\frac{\delta^{\rm I}}{\delta_0\Lambda L_N^2}\right|_{\text{peak value}}=\frac{R^2E}{\pi G}(2.76/\gamma^2)\left[\frac{(\gamma-1)(\gamma^2/3!-1)}{2}-0.38\right], \tag{47}$$

which clearly indicates that the peak value of the hysteretic dislocation damping that is represented by $\delta^{\rm I}$ versus the strain-amplitude plot depends upon the concentration of the weak obstacles along the dislocation line. This dependence is almost linear for the value of γ greater than about 5, which means on the average four obstacles per network length. Hence

$$\left.\frac{\delta^{\rm I}}{\delta_0\Lambda L_N^3}\right|_{\text{peak value}}\cong R^2(E/\pi G)0.23N_{\rm ob}^d,\quad \gamma>5\,. \tag{48}$$

In Fig. 1 the amplitude-dependent–only logarithmic decrement denoted by $\delta^{\rm I}$ is plotted with respect to the normalized applied uniaxial stress amplitude σ_0/Γ_c for various values of the number of weak pinning obstacles, γ using the plotter facilities of an HP-9821A minicomputer for a single crystal. In this example we have selected $|R(\theta,\phi)|=\frac{1}{2}$, which corresponds to the best orientation of the active dislocation slip system with respect to the uniaxial stress system. There are two important features associated with these plots: firstly, the fact that the maximum in the decrement (hysteretic in origin) occurs at about $\sigma_0/\Gamma_c=1.5$ regardless of the value of γ, which yields $q_{\max}=1.33$ as an excellent agreement with the analytical result of 1.3 obtained from Eq. (46) previously. Secondly, the nonlinear behavior of the decrement in regard to its dependence on the obstacle density extends up to the value of $\gamma=50$ (approximately).

D. Linear frequency-dependent region

The logarithmic decrement related to the out-of-phase contribution to the strain denoted by Eq. (42) can be formulated in the following:

$$\frac{\delta^{\rm II}}{\delta_0\Lambda L_N^2}=\frac{R^2E}{\pi G}\Omega_{B,N}Z(\gamma,q_0)\Big|_{q_0=\Gamma_c/|R|\sigma_0}\,, \tag{49}$$

where

$$Z(\gamma,q_0)\equiv\gamma^{-4}q_0\int_{q_0}^{\infty}[F(\gamma,q)+F(\gamma,q_0)](q^2-q_0^2)^{1/2}\frac{dq}{q^3}\ , \tag{50}$$

and according to Eq. (42)

$$F(\gamma,q)\equiv 5!\left\{1+e^{-q}\left[\gamma^4(\gamma-1)\frac{q+1}{5!}-\left[\sum_0^5\frac{q^m}{m!}\right]-(\gamma-1)(q+1)\right]+(\gamma-1)(q+1)\left[\sum_0^5\frac{q^m}{m!}\right]e^{-2q}\right\}, \tag{51}$$

for $q<\gamma$; otherwise $\gamma\rightarrow q$ (replacement operation) using the relations (6) and (7). Imposed restriction on the $F(\gamma,q)$ due to frozen-in loop distribution below the threshold can be eliminated rigorously by redefining the function $Z(\gamma,q_0)$ as such

$$Z(\gamma,q_0)\,|_{q_0<\gamma}\equiv\gamma^{-4}q_0\left[\int_{q_0}^{\infty}[F(\gamma,q)+F(\gamma,q_0)](q^2-q_0^2)^{1/2}\frac{dq}{q^3}+\int_{\gamma}^{\infty}[F(\gamma,\gamma)-F(\gamma,q)](q^2-q_0^2)^{1/2}\frac{dq}{q^3}\right] \tag{52}$$

and

$$Z(\gamma,q_0)\,|_{q_0>\gamma}=\gamma^{-4}q_0 2F(\gamma,\gamma)\int_{q_0}^{\infty}(q^2-q_0^2)^{1/2}\frac{dq}{q^3}\ . \tag{53}$$

The integral in Eq. (53) can be easily evaluated which yields

$$Z(\gamma,q_0)=(\pi/2)\gamma^{-4}F(\gamma,\gamma),\quad q_0\geq\gamma \tag{54}$$

and clearly tells us that the frequency-dependent part of the logarithmic decrement is independent from the stress amplitude below the threshold stress level as it should be according to our physical model of the breakaway process.

The above integrals may be reduced into the Weyl fractional integral transform[15] which, however, in the present case does not yield any complete analytical solution in terms of the well-known special functions. For analytical as well as the numerical procedure conveniences the function given by Eq. (51) may be separated into the following two terms which are capable of representing the linear frequency dependence (for moderate stress amplitudes) of the damping behavior of the dislocation plus the dragging impurity system for large and small obstacle densities efficiently, respectively. This separation into terms becomes more transparent for the obstacle densities, $\gamma>10$ (approximately). Otherwise, for low obstacle densities both terms should be considered simultaneously. Hence one can write

$$F(\gamma,q)=F_1(\gamma,q)+F_2(\gamma,q)\ , \tag{55}$$

where

$$F_1(\gamma,q)=5!(\gamma^4/5!-1)(\gamma-1)(1+q)e^{-q} \tag{56}$$

and

$$F_2(\gamma,q)=5!\left[1-e^{-q}\sum_0^5(q^m/m!)\right], \tag{57}$$

where $q\leq\gamma$. Using the above definition in connection with Eq. (52), one can write

$$Z(\gamma,q_0)=Z_1(\gamma,q_0)+Z_2(\gamma,q_0)+R(\gamma,q_0)\ , \tag{58}$$

where

$$Z_1(\gamma,q_0)=(5!/\gamma^4)(\gamma^4/5!-1)(\gamma-1)\times[(1+q_0)e^{-q_0}\pi/4+q_0L_0(q_0)+L_1(q_0)] \tag{59}$$

and

$$Z_2(\gamma,q_0)=\frac{5!}{\gamma^4}\left[\left[2-e^{-q_0}\sum_0^5\frac{q_0^m}{m!}\right]\frac{\pi}{4}-q_0\sum_0^5\frac{L_n(q_0)}{n!}\right], \tag{60}$$

here $L_n(z)$ is a new class of special functions which can be represented by

$$L_n(z)\equiv\int_z^{\infty}x^{n-3}e^{-x}(x^2-z^2)^{1/2}dx \tag{61}$$

or

$$L_n(z)=\tfrac{1}{2}\int_{y=z^2}^{\infty}x^{n/2-2}e^{-\sqrt{x}}(x-y)^{1/2}dx\ , \tag{62}$$

which is closely related to the Weyl fractional integral transform of the function denoted by $x^{n/2-2}\exp(-\sqrt{x}\,)$. The function $R(\gamma,q_0)$ which appears in Eq. (58) is corresponding to the following term:

$$R(\gamma,q_0)=\left[F(\gamma,\gamma)\int_{\gamma}^{\infty}(q^2-q_0^2)^{1/2}\frac{dq}{q^3}-\int_{\gamma}^{\infty}F(\gamma,q)(q^2-q_0^2)^{1/2}\frac{dq}{q^3}\right], \tag{63}$$

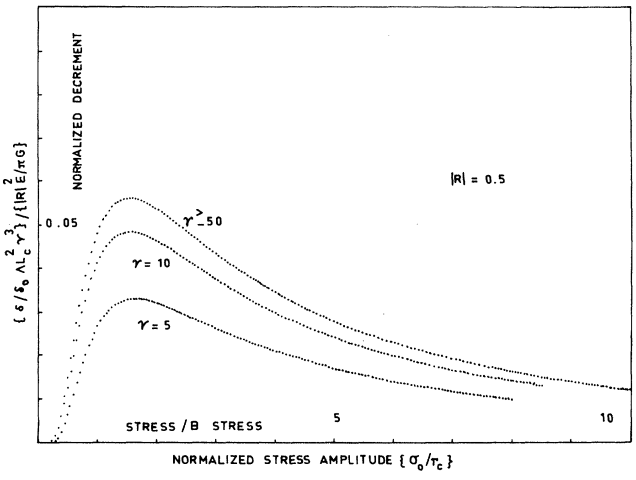

FIG. 1. Amplitude-dependent–only logarithmic decrement δ^I is plotted with respect to the normalized applied stress amplitude for various values of the number of weak pinning points γ. The decrement has been normalized to the factor $\delta_0\Lambda L_c^2$, where δ_0 is a constant of order of unity, Λ is the dislocation density, and L_c is the mean loop length between the weak obstacles (linear frequency region).

which has a negligible contribution to the decrement for medium and high stress-amplitude regions, especially large values of γ about 10 therefore will not be considered for our subsequent discussion.

Only for two special cases, $n=3$ and $n=4$, does one have the following simple results in terms of the well-known "modified Bessel functions" of orders of 1 and 2, respectively:

$$L_3(z)=zK_1(z)$$

and (64)

$$L_4(z)=z^2K_2(z)\ .$$

Otherwise, it seems that there is no simple and direct connection between these two classes of special functions.

For small values of q_0, the large stress amplitudes, using the definition of the γ functions in connection with Eq. (59), one obtains $L_n(q_0)\rightarrow(n+2)!$ for $n>1$. With the use of the properties of $L_n(z)$, the following important and useful relationships can be written for medium and large values of the stress amplitudes, respectively.

(a) Small stress amplitudes: $\lim[Z_1(\gamma,q_0)]\rightarrow 0$; when $q_0\rightarrow\infty$.

(b) Small stress amplitudes: $\lim[Z_2(\gamma,q_0)]\rightarrow(5!/\gamma^4)\times\pi/2$; $q_0\rightarrow\infty$.

(c) Large stress amplitudes: $\lim[Z_1(\gamma,q_0)]\rightarrow(5!/\gamma^4)\times(\gamma^4/5!-1)(\gamma-1)(1+\pi/4)$; $q_0\rightarrow 0$.

(d) Medium stress amplitudes: $\lim[Z_2(\gamma,q_0)]\rightarrow(5!/\gamma^4)\times(\pi/16)q_0$; $5<q_0<0.1$.

(e) Large stress amplitudes: $\lim[Z_2(\gamma,q_0)]\rightarrow(5!/\gamma^4)\times 6.7E-3$; when $q_0<0.04$.

In Fig. 2 the frequency-dependent part of the decrement denoted by δ^{II} is plotted with respect to the normalized stress amplitude on a double-logarithmic scale using Eq. (49) for the numerical-integration procedure. It can be demonstrated that for the small number of obstacles the dominant contribution comes from the term denoted by $Z_2(\gamma,q_0)$ which also shows a large region of amplitude-independent behavior as can be easily anticipated from Fig. 3. For the large obstacle densities the $Z_1(\gamma,q_0)$ term becomes very pronounced and almost determines the whole damping behavior (for the linear frequency range) for $\gamma>10$, and it is a monotonically increasing function of the stress amplitude.

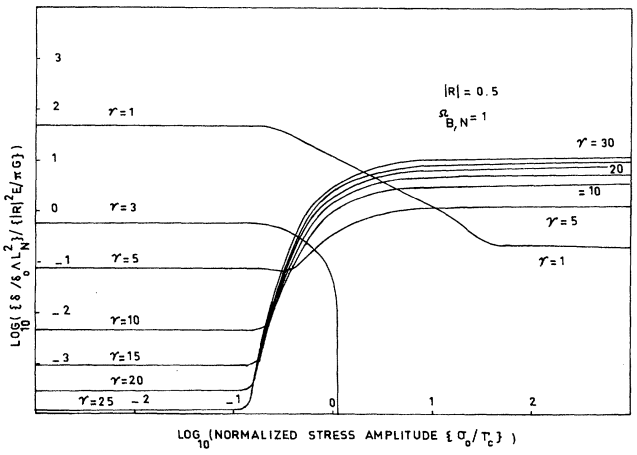

FIG. 2. δ^{II} is the frequency-dependent part of the logarithmic decrement which is plotted with respect to the normalized applied stress amplitude for the various values of the number of weak pinning points per network length denoted by γ, where the normalization frequency $\Omega_B=\omega/\omega_B^0$ is taken to be equal to unity as an example. Here ω_B^0 is the fundamental frequency of the dislocation loop of length L_c in the absence of the inertial term (Ref. 13) and it is given by $C\pi^2/BL_c^2$.

Our extensive computer experiments indicated that the following analytical expression can be used very effectively for the small stress-amplitude region which has an upper bound as $\sigma_0|R|/\Gamma_c<0.25$:

$$\frac{\delta^{II}}{\delta_0\Lambda L_N^2}=\frac{R^2E}{\pi G}\Omega_{B,N}5!\gamma^{-4}\left[\left[\frac{\gamma^4}{5!}-1\right](\gamma-1)\frac{q_0\pi e^{-q_0}}{4}+\frac{\pi}{2}\right], \tag{65}$$

and similarly for the large stress-amplitude region which can be defined by the following inequality: $\sigma_0|R|/\Gamma>5$. The following asymptotic expression yields a very accurate result. [In Eq. (66) when $\sigma_0|R|/\Gamma>25$, the $\pi q_0/16$ term should be replaced by a constant which is given by $6.7E-3$]:

$$\frac{\delta^{II}}{\delta_0\Lambda L_N^2}=\frac{R^2E\Omega_{B,N}}{\pi G}5!\gamma^{-4}\times\left[\left[\frac{\gamma^4}{5!}-1\right](1+q_0)e^{-q_0}\frac{\pi}{4}+\frac{\pi}{16}q_0\right]. \tag{66}$$

In Fig. 3 the functions $Z_1(\gamma,q_0)$ and $Z_2(\gamma,q_0)$ are plotted using the numerical integrations of Eqs. (59) and (60), as a function of $\sigma_0|R|/\Gamma$ where $R=\frac{1}{2}$, in a double-logarithmic scale. For the most critical region where depinning occurs one has to use the full analytical expression

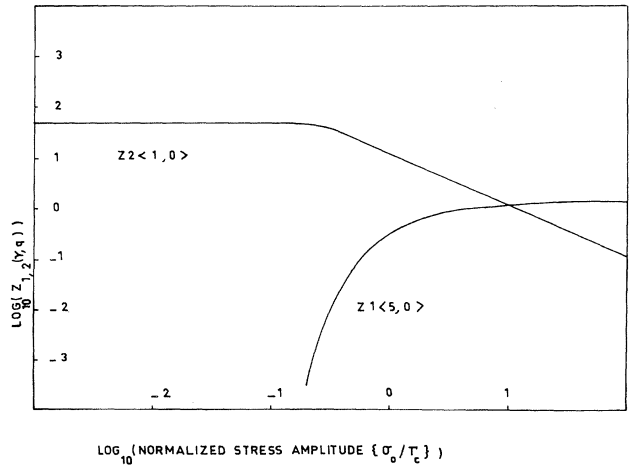

FIG. 3. $Z_1(5,q_0)$ and $Z_2(5,q_0)$ functions are plotted with respect to the normalized stress amplitude σ_0/Γ_c on a double logarithmic scale using a numerical integration procedure. Where $\Gamma_c=\pi f_m/4aL_c$, f_m is the maximum pinning force.

$(0.5 < \sigma_0 \mid R \mid /\Gamma < 5)$ to obtain accurate and meaningful results. Otherwise, the above equation denoted by (66) yields good numerical values especially for moderate and high $\gamma > 5$ for this special region of main interest.

IV. DISCUSSION

In Fig. 4 the logarithmic decrement for the linear frequency region $\delta = \delta^{I} + \delta^{II}$ is plotted with respect to the normalized stress amplitude σ_0/Γ_c for various values of the normalized frequency denoted by $\Omega_{B,N}$ and the number of weak pinning points per network length γ on a double-logarithmic scale. This plot immediately reveals the existence of the two regions, the stress-amplitude independent and dependent, respectively. The stress-amplitude–independent region as well as the very high-stress-amplitude range are completely dominated by the dragging point-defect–associated dislocation damping. However, at the medium-stress level where the repinning process becomes the rate determining step the damping is almost frequency insensitive. Again the peak in the decrement occurs which is hysteretic in origin at about $\sigma_0/\Gamma_c = 1.5$ regardless of the value of γ.

The most interesting feature of the whole dislocation damping phenomena in the presence of the dragging point defects plus the weak obstacles can only be deduced from the rigorous and the exact numerical integration solution of the expression denoted by Eqs. (37) and (38). In Fig. 5 the logarithmic decrement obtained from the rigorous solution is presented as a function of the normalized stress amplitude σ_0/Γ_c for various values of the normalized frequency Ω_B and using two different obstacle densities. This plot indicates the existence of the three distinct stages as far as the stress-amplitude dependence is concerned: the stress-amplitude–independent low-stress levels, the depinning-controlled transition region of medium-stress level, and the stress-amplitude–insensitive stage of large-stress levels. The maximum in the decrement occurs at exactly $\Omega_B = 0.1$ normalized frequency with respect to the

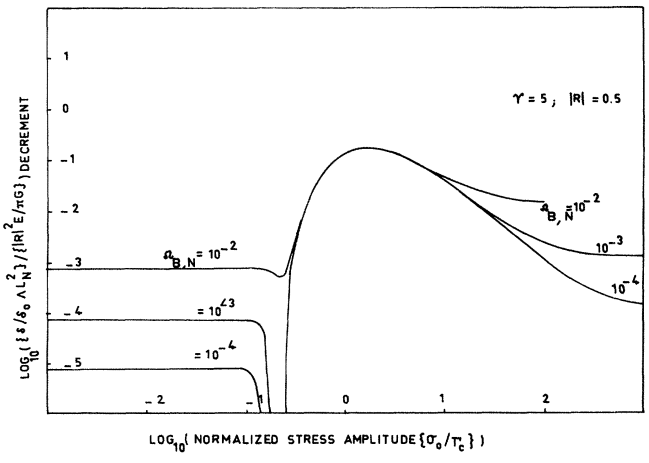

FIG. 4. Total logarithmic decrement $\delta = \delta^{I} + \delta^{II}$ is plotted according to Eqs. (37) and (38) with respect to the normalized stress amplitude on a double logarithmic scale for the various values of the normalized frequency.

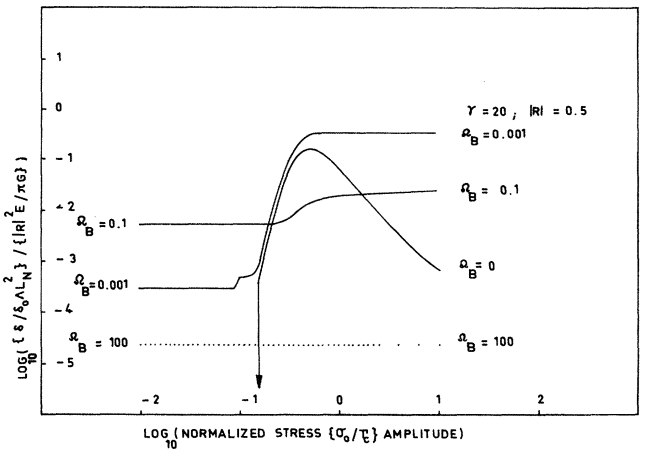

FIG. 5. Total logarithmic decrement according to the rigorous theory is plotted using a numerical integration procedure as a function of the normalized stress amplitude for different values of the normalized frequency $\Omega_{B,N}$.

mean loop length L_c of the dragging point defects at the stress-amplitude–independent stage, respectively. In the depinning stage there is a continuous transformation from this peak into another one with a maximum normalized frequency of $\Omega_{B,N} = 1$, which corresponds to $\Omega_B = 1/\gamma^2$. Close inspection of Eq. (38) clearly reveals the fact that at the end of the depinning process all the dislocation segments will be accumulated at the network length L_N which has a sharp relaxation maximum at exactly $\Omega_{B,N} = 1$ due to the δ distribution function of the segment length. According to Oğurtani in a previous observation,[13] the dragging peak in the stress-amplitude–independent region shows a maximum when $\Omega_B = 0.1$ for a random distribution of the dislocation segment lengths. At the depinning stage the maximum in the decrement can be easily observed for very low normalized frequency values which yields $\sigma_0/\Gamma_c = 0.5$ regardless of the magnitude of γ. This value of the depinning effective stress amplitude is a factor of 3 smaller than the one obtained previously using the nonrigorous solution of the problem. As we mentioned earlier the nonrigorous solution employs a distribution function which is rather crude at medium and high-stress-amplitude regions.

At the high-stress-amplitude stage where the depinning process nears completion, again decrement becomes very insensitive in regard to the variations in the normalized frequency. However, for very low frequencies sensitivity starts to reappear, and the decrement decreases with the stress amplitude.

The effect of pinning-point density which is denoted by γ follows similarly as discussed previously in connection with Fig. 2. Solely, the increase in the obstacle density results decrease in the peak height in stage I and causes just the opposite effect on stages II and III, respectively.

The temperature dependence of the amplitude as well as the frequency-dependent dislocation damping could arise through three distinct and important factors according to the present model calculations. The first factor is the temperature dependence of the drag coefficient B which is introduced by Eq. (23a) and fully developed in the Appen-

dix. The second factor which also causes variations in the decrement with temperature is due to the concentration of the weak obstacles N_{ob}^{d} along the dislocation line through the parameter γ. This concentration shows also the Langmuir-type adsorption isotherm described by its own binding energy. The third but the most important contribution to the temperature dependence might come from Γ_c, the depinning stress, through the factor f_m, which has been called as the maximum depinning force. The temperature dependence of f_m may be represented by $f^{\infty}\exp(H_{ob}^{dp}/kT)$ above the softening temperature, where H_{ob}^{dp} is the depinning activation enthalpy. However, a better description can be given by the following *ad hoc* expression which takes care of the hard as well as the soft interaction modes through thermal fluctuations simultaneously:

$$f_m = f_m^0[1+(f_m^0/f_m^{\infty})\exp(-H_{ob}^{dp}/kT)]^{-1}, \tag{67}$$

which indicates that the thermal activation of the depinning process below a certain characteristic temperature will be almost frozen-in and cannot show any temperature variation. Hence similarly one can write

$$\Gamma_c = \Gamma_c^0[1+(\Gamma_c^0/\Gamma_c^{\infty})\exp(-H_{ob}^{dp}/kT)]^{-1}, \tag{68}$$

where f_m^0 and Γ_c^0 are the depinning force and the stress at absolute temperature, respectively. f_m^{∞} and Γ_c^{∞} are the similar quantities at the infinite temperature. The relationship between Γ_c and f_m are as follows: $\Gamma_c = \pi f_m/4aL_c$, and it was mentioned previously that the exact nature of this expression depends upon the specific model of force calculation on the pinning point due to bow-out dislocation segment.

In Fig. 6 the logarithmic decrement obtained from the rigorous solution is plotted as a function of the homologous temperature T/T_m for various values of the stress amplitude, the obstacle density, and the excitation frequency, respectively, on a double logarithmic scale. In this universal plot the energies such as H_i', $E_{i,b}$, and H_{ob}^{dp} are all normalized with respect to kT_m, where T_m is the melting temperature and k is Boltzmann's constant. With the adopted normalization procedure one can easily investigate the general behavior of the system without referring to any specific material parameters. In Table I our extensive finding in regard to the numerical experiments are

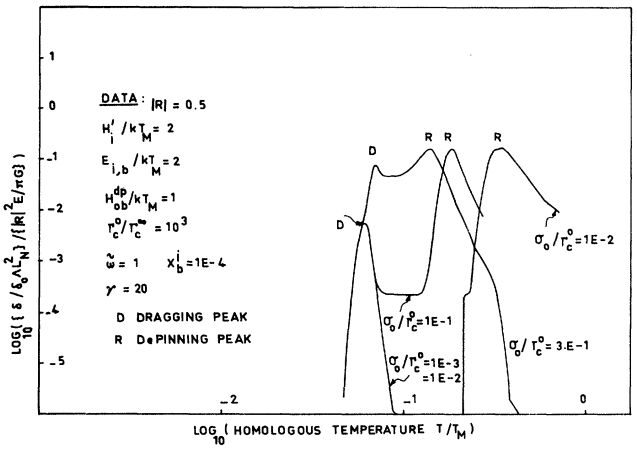

FIG. 6. Total logarithmic decrement according to the rigorous theory is plotted as a function of the homologous temperature T/T_M for various values of the normalized stress amplitude and the excitation frequency using two different obstacle densities.

presented in terms of the peak position and the peak height. Figure 6 clearly reveals the existence of two distinct peaks in the internal friction versus homologous temperature plots. The first peak which appears at the low-temperature side is due to the dragging point defects and it has the nature of viscous damping as can be anticipated from its strong frequency dependence and the stress-amplitude independence. The second peak which is rather skew on the high-temperature side shows strong stress-amplitude dependence in regard to its peak position and complete insensitivity with respect to the variations in the excitation frequency. This second peak is closely related to the depinning process of the dislocation segment from the weak obstacles, and its height increase with the increase in the obstacle density. On the other hand, the dragging peak shows just the opposite behavior with respect to the similar variations in the density of the weak obstacles. For high values of the stress amplitude these two peaks start to overlap considerably.

In order to investigate the global behavior of the dislo-

TABLE I. General behavior of the internal friction peaks associated with the dislocation damping in the presence of the dragging point defects plus the weak obstacles on a homologous temperature plot. I corresponds to stage I (stress independent), II corresponds to stage II, the transition region. "*S*" means that the effect of saturation hinders the variations.

		Increase in stress amplitude		Increase in excitation freq.	Increase in obstacle density	Increase in drag conc.
Dragging peak		I	II			
	Peak position		↓	↑	↑	↑ or *S*
	Peak height		↑		↓	
Depinning peak						
	Peak position	↓	↓			
	Peak height			↓ at very high Ω_B	↑	↓ or *S*

cation damping phenomena in regard to the variations in the excitation frequency ω we have adopted the following frequency renormalization procedure using Eqs. (27) and (A10):

$$\Omega_{B,N}=\frac{\omega BL_N^2}{\pi^2 C}\equiv\tilde{\omega}\tilde{\tau}\ , \tag{69}$$

where

$$\tilde{\omega}\equiv\left[10^{12}\frac{\omega L_N^2 kT_M}{\pi^2 CbD'_{i,0}}\right] \tag{70}$$

and

$$\tilde{\tau}\equiv\left[10^{-12}\frac{(T/T_M)3\exp(H'_i/kT)}{1+3(X_i^b)^{-1}\exp(-E_{i,b}/kT)}\right]\ . \tag{71}$$

In Fig. 7 the strain-amplitude–dependent decrement for a polycrystalline material is plotted assuming that the material is elastically isotropic and individual grains are randomly distributed employing Eqs. (10) and (43), respectively. This plot immediately reveals the fact that in a polycrystalline sample the depinning peak shows a substantial amount of reduction in the height, and as well for the large skewness on the high stress-amplitude side (or high-temperature side on the homologous temperature plot) of the maxima.

ACKNOWLEDGMENT

The authors wish to thank Professor T. S. Ke and Professor H. Schultz for valuable discussions.

APPENDIX: THERMAL EQUILIBRIUM SEGREGATION ON DISLOCATIONS

The statistical thermodynamics of a solution of point defects of a single type which do not interact is the simplest possible case to consider. We write the small canonical partition function Q^d

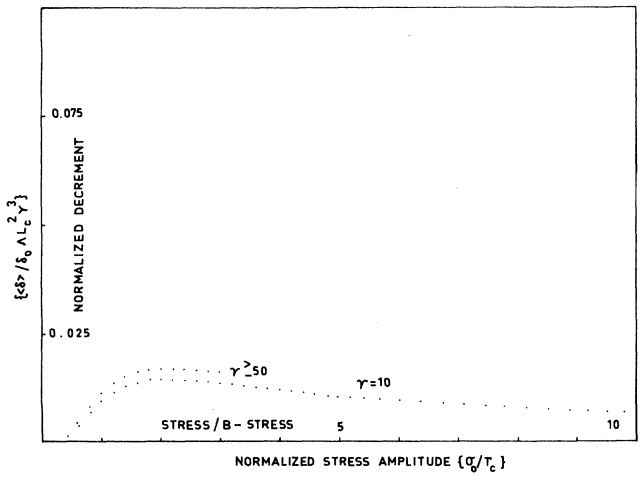

FIG. 7. Frequency-independent part of the decrement is plotted with respect to the normalized stress amplitude for a polycrystalline sample (elastic isotropy) for two different values of the weak obstacle densities.

$$Q^d=(N_i^d!)^{-1}\sum_{j\ (\text{states})}\exp(-E_j^{b,d}/kT)\ , \tag{A1}$$

where N_i^d is the number of interstitials distributed over $N_i^{d,0}$ available sites at the dislocation and γ is the ratio of interstices to regular lattice sites, $E_j^{b,d}$ is the energy of state j, and the summation is over all states but with the specific condition that no more than one interstitial occupied a site. Using the usual maximum-term method, we find that

$$\mu_i^d=-kT\ln\frac{1-\theta_i^d}{\theta_i^d}+E_i^{b,d}\ , \tag{A2}$$

where $\theta_i^d=N_i^d/N_i^{d,0}$. One can write exactly the same relationship for the bulk phase. Thermochemical equilibrium between the dislocation region and the bulk phase in regard to the chemical species i requires that

$$\mu_i^d=\mu_i^b \tag{A3}$$

or

$$-kT\ln\left[\frac{1-\theta_i^b}{\theta_i^b}\right]+E_i^{b,b}=-kT\ln\left[\frac{1-\theta_i^d}{\theta_i^d}\right]+E_i^{b,d}\ , \tag{A4}$$

which after arranging the terms yields

$$\frac{\theta_i^d}{1-\theta_i^d}=\frac{\theta_i^b}{1-\theta_i^b}\exp\left[\frac{E_{i,b}}{kT}\right]\ , \tag{A5}$$

where $E_{i,b}=E_i^{b,b}-E_i^{b,d}$ is the enthalpy of binding of the interstitial species to the dislocation line. The relationship between θ_i and the atomic fraction X_i is as follows:

$$X_i=\frac{\theta_i}{\theta_i+1/\gamma}\ , \tag{A6}$$

where γ is the ratio of interstices to the regular lattice sites, and it is equal to 3 and 6 for the octahedral and the tetrahedral sites in a bcc lattice, respectively. For dilute interstitial solid solutions the atomic fraction in the bulk phase may be taken as $X_i^b\cong\gamma\theta_i^b$ as a good approximation. Hence one can write

$$\theta_i^d\cong\left[1+\left[\frac{\gamma}{X_i^b}\right]\exp\left[\frac{-E_{i,b}}{kT}\right]\right]^{-1}\ , \tag{A7}$$

which shows a 50% saturation temperature T_s, and it may be obtained from the following expression:

$$T_s\cong-E_{i,b}/k\ln(X_i^b\gamma^{-1})\ . \tag{A8}$$

One can also obtain an exact expression for T_s without making any dilute solution approximation using Eq. (A5) directly which results in

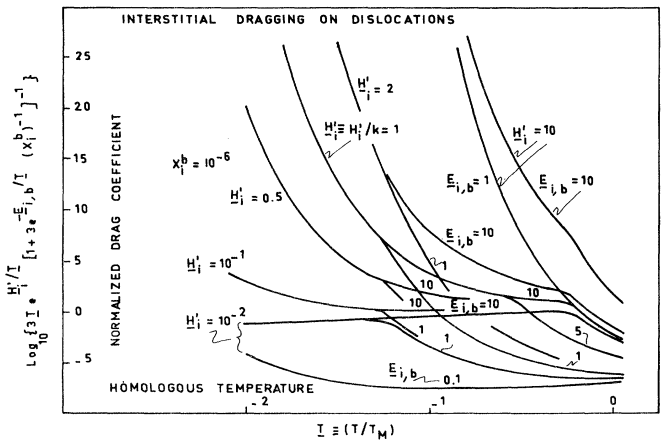

FIG. 8. Normalized mobile impurity drag coefficient is plotted for various values of the enthalpy of diffusion and the binding energy as a function of the homologous temperature for the bulk atomic fraction $X_i^b = 10^{-6}$.

$$T_s = -\frac{E_{i,b}}{k \ln[\theta_i^b/(1-\theta_i^b)]} \,. \tag{A9}$$

Now if one combines Eq. (A7) with Eq. (23a) the following relationship can be deduced:

$$B = B_0 + kTb^2 \pi n_L D_{i,0}'^{-1} \frac{\gamma \exp(H_i'/kT)}{1+\gamma(X_i^b)^{-1}\exp(-E_{i,b}/kT)} \,, \tag{A10}$$

where n_L is the density of regular lattice sites which is equal to $2/a^3$ for a bcc metal and H_i' is the enthalpy of migration of the interstitial impurities in the vicinity of the dislocation core region (see Fig. 8).

The temperature dependence of the damping coefficient associated with the mobile point defects can be easily obtained from Eq. (A10) which yields the following expression exactly for the complete range of temperatures:

$$Q_{\text{eff}} = \frac{d \ln(B^{\text{imp}}/T)}{d(1/kT)} = H_i' + \frac{E_{i,b}}{1+\gamma^{-1}X_i^b \exp(E_{i,b}/kT)} \,, \tag{A11}$$

which yields $Q_{\text{eff}} = H_i'$ well below the saturation temperature and results with $Q_{\text{eff}} = H_i' + E_{i,b}$ similarly above that temperature. Therefore, the apparent activation energy of the process shows very large temperature dependence or broadening if the peak temperature lies in the vicinity of the saturation temperature T_s.

[1]J. S. Koehler, in *Imperfection in Nearly Perfect Crystals*, edited by W. Shockley, J. H. Hollomon, R. Mauerer, and F. Seitz (Wiley, New York, 1952).
[2]A. V. Granato and K. Lücke, J. Appl. Phys. 27, 583 (1956); 27, 789 (1956).
[3]L. J. Teutonico, A. V. Granato, and K. Lücke, J. Appl. Phys. 35, 220 (1964).
[4]M. Koiwa and R. R. Hasiguti, Acta Metall. 13, 1219 (1965).
[5]P. Peguin and H. K. Birnbaum, J. Appl. Phys. 39, 4428 (1968).
[6]K. Lücke, A. V. Granato, and L. J. Teutonico, J. Appl. Phys. 39, 5181 (1968).
[7]H. M. Simpson and A. Sosin, Phys. Rev. B 5, 1382 (1972).
[8]H. M. Simpson, A. Sosin, and D. F. Johnson, Phys. Rev. B 5, 1393 (1972).
[9]R. Klam, H. Schultz, and H. E. Schaefer, Acta Metall. 28, 259 (1980).
[10]R. B. Schwarz, Acta Metall. 29, 311 (1981).
[11]A. Seeger, J. Phys. (Paris) Colloq. C5, Suppl. 10, 201 (1981).
[12]G. Fantozzi, C. Esnouf, W. Benoit, and I. G. Ritchie, Prog. Mater. Sci. 27, 311 (1982).
[13]T. Ö. Oğurtani, Phys. Rev. B 21, 4373 (1980).
[14]E. Abramowitz and I. Stegun, *Handbook of Mathematical Functions* (Dover, New York, 1968), p. 227.
[15]A. Erde'lyi, *Tables of Integral Transform* (McGraw-Hill, New York, 1954), Vol. II, p. 201.